Eur. Phys. J. D (2020) 74: 72
https://doi.org/10.1140/epjd/e2020-100526-1

THE EUROPEAN PHYSICAL JOURNAL D

Regular Article

Monte Carlo simulation of RF breakdown in oxygen – the role of attachment*

Marija Puač[1,a], Antonije Đorđević[2,3], and Zoran Lj Petrović[1,2]

[1] Institute of Physics, University of Belgrade, Pregrevica 118, 11080 Belgrade, Serbia
[2] Serbian Academy of Sciences and Arts, Knez Mihailova 35, 11001 Belgrade, Serbia
[3] School of Electrical Engineering, University of Belgrade, Bulevar kralja Aleksandra 73, 11001 Belgrade, Serbia

Received 25 October 2019 / Received in final form 22 February 2020
Published online 14 April 2020

Abstract. Breakdown in oxygen, in external radio-frequency (RF) electric field is analyzed by employing a Monte Carlo simulation (MCS). Results were obtained for 13.56 MHz and distance between electrodes of 15 mm. Physical background of an oxygen RF breakdown is explained by observing time-resolved spatial distributions of electron concentration, mean energy, elastic scattering rate, ionization rate and attachment. The role of attachment is investigated in cases when these processes are included and when they are not. Especially influence of the attachment is highlighted by comparing oxygen and argon breakdown-voltage curves and spatial profiles. The electron losses induced by attachment extend the motion of the electron prebreakdown swarm much closer to electrodes to achieve a greater production; hence, spatial profiles at high values of the product pd where p is the pressure and d is the gap between electrodes, become more similar to those at the minimum of the breakdown curve. The most striking difference between the breakdown curves in argon and in oxygen is in the high increase of the breakdown voltage for high pd in oxygen.

1 Introduction

Considering the applicability of radio-frequency (RF) plasmas and their wide presence in industry, from integrated circuit (nanoelectronics) processing [1,2] all the way to the non-equilibrium (cold) plasma applications in medicine and agriculture [3,4], one would expect an equivalent interest in fundamental properties of RF breakdown and discharges. The basic understanding of RF plasmas that has been reached recently [5,6] is in principle relevant when the so called alpha regime is considered. However these studies start from a formed plasmas and consider the final profile of the self-consistent electric field. Thus those papers are not directly relevant for the breakdown which occurs in pristine gas without space charge and without preexisting excited species (that is the basic definition of the gas background in swarm studies). Since the operating voltage for formed plasmas may be quite different from the breakdown condition and since the whole art of producing the non-equilibrium plasmas at atmospheric pressure depends very much on controlling the breakdown condition it is important that the understanding of RF plasma operation is being matched by the studies of RF breakdown [7–10] that have been undertaken recently.

While the RF discharges have been studied for quite some time by the likes of Tesla, Hittorf, Pupin and others, the swarm limit that is relevant for the breakdown conditions has not been considered for some time, although motivation existed in propagation of the electromagnetic waves through the ionosphere. In 1946 Holstein published a research on electron energy distribution in high-frequency gas discharge [11]. This study falls to the category of swarm physics and is thus directly relevant for breakdown but in itself is not a study of breakdown conditions. Later, the basic research of high-frequency breakdown was done by Margenau and Hartman and was published in their four papers named "Theory of high-frequency gas discharges", including calculations of electron distribution functions, breakdown at low pressures and similarity laws [12–15]. At the same time, von Engel was investigating the starting potentials of high-frequency gas discharges and he proposed a theory (though we could use the term phenomenology in its literal meaning) of the high-frequency breakdown that has not been significantly changed almost to the present day [16,17]. The basic idea in the proposed explanation by von Engel and coworkers is that the condition for breakdown coincides with

* Contribution to the Topical Issue "Low-Energy Positron and Positronium Physics and Electron-Molecule Collisions and Swarms (POSMOL 2019)", edited by Michael Brunger, David Cassidy, Saša Dujko, Dragana Marić, Joan Marler, James Sullivan, Juraj Fedor

[a] e-mail: smarija@ipb.ac.rs

the condition that in one half period electrons may drift from one electrode to the other and then drift back as the field changes direction. One of the reasons for the absence of RF breakdown research is probably the existence of only a few experiments that could measure breakdown-voltage curves with reasonable precision providing reliable and well defined results that could be used in modeling. One of the experimental setups that has produced a lot of results of breakdown-voltage curve measurements in different gases in recent times, is the experiment of Lisovskiy and coworkers [18]. In the analysis these authors directly apply von Engel's phenomenology and extract even drift velocities under assumption of a sinusoidal time dependence of the drift velocity with changing E/N (t). Recently, two more elaborate experiments have been constructed by Korolov and colleagues [9,10] and Đorđević et al. [19,20]. Hence, now there exists a better starting point to build models of RF breakdown.

Basic physical description of RF breakdown has already been provided in our previous papers [7,8] in case of argon as a background gas. Also, the shape of the breakdown-voltage curve with a double-valued region at low pressures and similarity law were explained. While argon was easy to analyze due to its simpler set of collisional processes, in this paper we chose oxygen as a target. Motivation for focusing on oxygen is that it is an important constituent of the atmosphere that adds attachment (two and three-body processes) as a new non-conservative channel for electron losses. Attachment, on the other hand defines breakdown (dielectric properties) and behavior of most atmospheric discharges (both natural and man-made).

Oxygen has (similar to nitrogen, the other dominant atmospheric gas) a number of rotational and vibrational excitations in addition to electronic excitations. As a consequence, losses of electron energy in gas are significant [21] at all energies as compared to argon. From the breakdown point of view, the attachment represents electron loss mechanism in the volume (in addition to the electron losses by electrode absorption). In oxygen it all occurs also in the background of higher energy losses but distribution function has to adjust to the conditions when ionization can overcome all the losses and thus breakdown has to occur at considerably higher E/N as compared to argon. In order to explain the role of the non-conservative electron losses on the breakdown in RF fields in the presence of vibrational excitation energy losses we shall compare the anatomy of the profiles of emission, energy and ionization to those of argon.

2 Model and Monte Carlo simulation

Monte Carlo (MC) code that we have used has been explained elsewhere [22,23]. In general, the code can keep track of any kind of particles (electrons, ions, neutrals metastables and photons) and at any time it registers fundamental characteristics of those particles, including their location, components of velocity and energy. At the beginning of simulation, electrons are initiated from the middle of the gap between the two electrodes and they start to move according to the applied external electric field. Electrons can experience collisions but, eventually, they hit electrodes and get absorbed (or possibly reflected). While colliding, electrons may produce new electrons through ionization. At the same time, ions are produced as well. At this point, any heavy particle (ions, metastables or neutrals) can be observed in the same manner as electrons. On the other hand, production of secondary electrons at electrodes (as consequence of heavy particles collisions with electrodes) is not needed to sustain RF discharges and breakdown due to electrons only is the basic mode of breakdown. Hence, we shall for the moment neglect the effect of heavy particles and also of photons. The fast neutrals and ions that play a critical role in the DC breakdown are of importance in RF only for very special circumstances. For most of the *pd* range the breakdown is purely determined by electrons only. Breakdown occurs in principle in the pristine, unperturbed, gas and thus populations of vibrationally excited molecules and metastables are negligible. On the other hand simulations for ions and other energetic heavy particles are quite demanding as for the computational time (due to order of magnitude different time scales required) with very little effects and only in a very narrow range of conditions. The role of heavy particles in RF breakdown will be addressed separately.

Apart from processes that occur in the gas volume, there are processes at surfaces of electrodes. Our code can include two types of surface collisions of electrons: reflections (elastic and inelastic, described by the reflection coefficient R), and the electron-induced secondary electron emission. Production of electrons by other processes may be quantified by gamma coefficients (yields) that can be, in theory, decomposed into a sum of contributions by ions, metastables, fast neutrals and photons [24]. Presently, however, these surface effects are neglected.

The cross sections for electron scattering in oxygen have been taken from Itikawa [21] with addition of the three-body attachment cross section that was taken from Phelps' LxCat database [25]. Results obtained by Itikawa's cross sections are presented in [26,27] while influence of the three-body attachment was analyzed in [28]. The pressure for simulations has been taken as 1 Torr. The results should be independent of the pressure (taking into account the frequency-pressure scaling), although with the three-body scaling for attachment there could be some pressure dependence and differences in profiles [28]. For the present conditions we could not find any significant effects due to the three-body attachment when pressure was varied from 1 Torr to 760 Torr.

3 Results and discussion

3.1 RF breakdown-voltage curve and time-resolved spatial distributions

The procedure used to determine breakdown conditions represented by the gas pressure and the corresponding breakdown voltage is explained in [7,8]. By employing that method, we have obtained the breakdown-voltage curve for oxygen presented in Figure 1a. The frequency

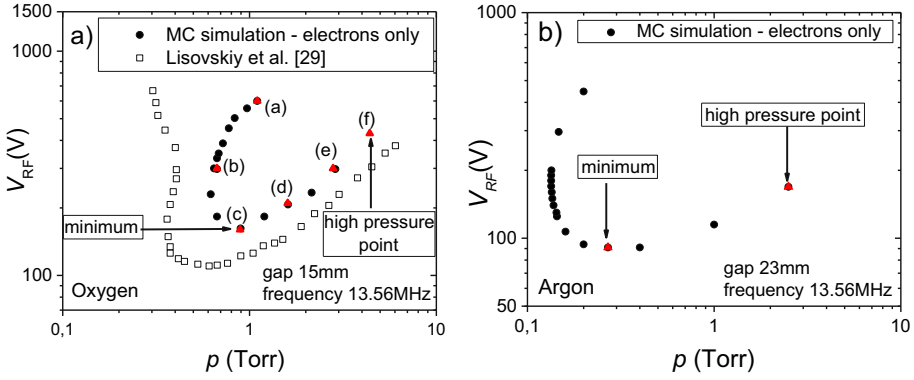

Fig. 1. Breakdown-voltage curves for RF breakdown at frequency of 13.56 MHz in different gases: (a) oxygen at electrode distance of 15 mm with available experimental data [29]; (b) argon at electrode distance of 23 mm [8]. Only electrons are included in MC simulation and there are no surface effects at electrodes, apart from absorption. Points in figure (a) marked from (a) to (f) are used as conditions for sampling presented in Figure 2.

of the external electric field is 13.56 MHz and the distance between the electrodes is 15 mm. Only electrons are included and their movement in gas and in the applied RF electric filed is observed. As there are no surface effects, electrons are removed from the simulation when they reach an electrode. Regarding the three-body attachment, it has been scaled with pressure (in Torr). As can be seen in Figure 1a, the breakdown curve has its characteristic "U" shape with a distinctive double-valued region where two breakdown voltages correspond to one breakdown pressure. Nature of this double-valued area is discussed and explained (for argon) in our previous papers [7,8].

In Figure 2 we present time-resolved spatial distributions of electron concentration, mean energy and rates of elastic scattering, ionizations and attachment for conditions marked with (a)–(f) in Figure 1a. Light blue lines describe the applied electric field. Having a closer look at the concentration of electrons, we can see that the swarm of electrons nicely follows the applied electric field and changes its direction of motion when the field changes its sign (passes through zero). Also, if we observe the changes from point (a) to point (f), electrons are being slowly pushed away from the electrodes, causing a smaller and smaller area of the electron cloud profile to overlap with the electrodes (the overlap represents losses at electrodes). This change leads to a decrease in electron losses by electrode absorption, which is manifested as a decrease in the breakdown voltage in the curve in Figure 1a. As expected, rates of elastic scattering and ionization follow the profiles of the mean energy. By comparing the ionization and concentration, we can see that an increase in concentration is a direct consequence of the maximum in the number of ionizations. The rate of attachment that includes both two- and three-body processes has a small interruption when the applied field is zero, while the ionization is perturbed much more.

By looking at Figures 1a and 2 it is easy to understand the shape of the RF breakdown-voltage curve in oxygen. If we move from the minimum of the curve, as an optimal breakdown condition, to lower pressures, there is a sharp increase in voltage. This increase exists due to a bigger and bigger overlap of the electron cloud with the electrodes, leading to larger and larger electron losses. Moving towards higher pressures from the minimum point, there is also an increase of breakdown voltage, but this increase is less dependent on the losses at electrodes and more on the losses in the gas volume due to the electron attachment.

3.2 Comparison of RF breakdown in argon and oxygen

A good way to understand how the attachment affects the oxygen RF breakdown is to compare these results to those obtained in argon [8]. To do so, we will first look at the breakdown-voltage curves for these two gases, presented in Figures 1a and 1b. Both curves are calculated for the applied frequency of 13.56 MHz. Despite the different distances between the two electrodes, 23 mm for argon and 15 mm for oxygen (chosen to be in accordance with some of the available experiments), they are close enough and conclusions could be drawn. The curves for both gases have a similar shape and distinctive minimums, but there is a considerable difference in the pd value and the breakdown voltage corresponding to the minimum. Oxygen discharge demands higher breakdown voltages and pressures to be maintained due to more electron excitation and vibrational collisions, requiring a higher E/N for electrons to reach the same mean energy. Of course, the presence of the attachment will push the breakdown towards even higher voltages to compensate for the resulting electron losses. The other difference is in the slope of the right-hand branch. From argon analysis [8] we know that at high pressures electrons are concentrated in the middle of the gap and losses at electrodes are very small. It is expected that the attachment, as a loss mechanism (together with the vibrational excitation as an energy loss), can be responsible for a sharp increase in breakdown voltages and the slope of the curve as a function of pd in the case of oxygen. We will verify this further by examining various time-resolved spatial profiles of the properties of the electron swarm (Figs. 3–5) and later on by analyzing electron energy distribution functions (Fig. 6).

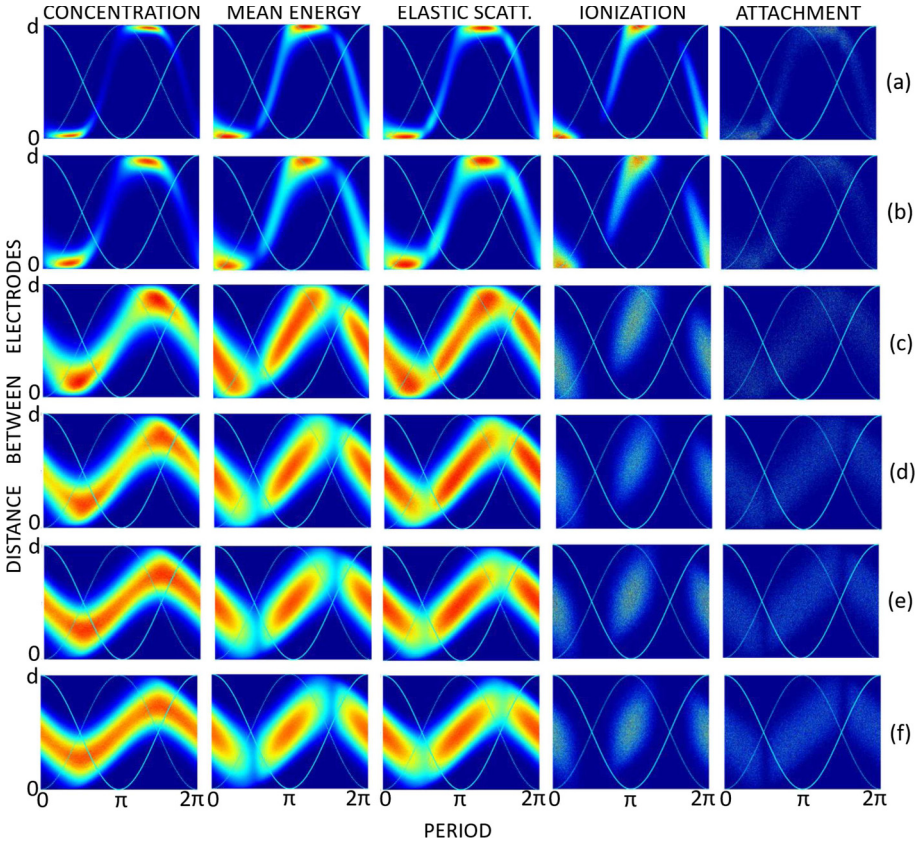

Fig. 2. Time-resolved spatial profiles of electron concentration, mean energy, elastic scattering, ionization and attachment rates for conditions marked in Figure 1. Light blue solid line represents applied field and light blue dotted line is the negative version of field profile to indicate direction of force on electrons. X-axis of plots are periods of time from 0 to π, while y-axis are distances between electrodes from 0 to $d = 15\,\text{mm}$. Background gas is oxygen, frequency of external electric field is 13.56 MHz and gap is 15 mm. Sampling time of all plots is the same so that qualitative and quantitative conclusions can be made.

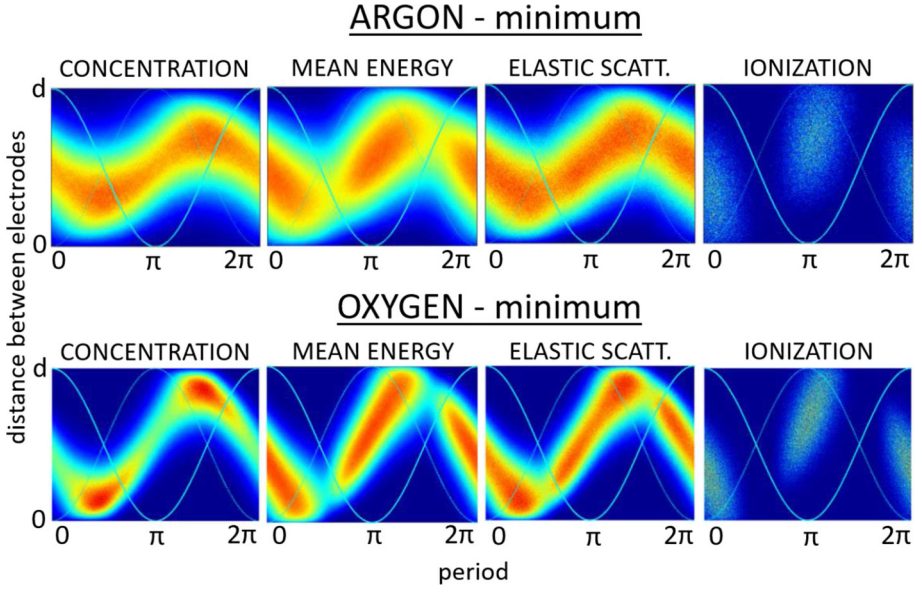

Fig. 3. Comparison of spatial profiles of electron concentration, mean energy and rates of elastic scattering and ionizations for two points that are minima of the breakdown-voltage curves (Fig. 1). Argon minimum: $V = 91\,\text{V}$ and $p = 0.27\,\text{Torr}$; oxygen: $V = 160\,\text{V}$ and $p = 0.89\,\text{Torr}$. X-axis of plots are periods of time from 0 to π, while y-axis are distances between electrodes from 0 to $d = 15\,\text{mm}$. In both cases sampling time is the same, so that quantitative comparison can be made.

In Figures 3 and 4 a comparison is presented of time-resolved spatial profiles for argon and oxygen at distinctive points of the breakdown-voltage curves, labeled in Figure 1 as "minimum" and "high pressure point". If we observe plots for conditions in minimums in Figure 3, they have similar modulations. In both cases the swarm of electrons is migrating from one electrode to the other one according to the applied field and only brushes the electrodes. Yet for oxygen, due to a higher pressure and higher losses, the growth towards the electrodes is more pronounced and the density peak is much sharper. Plots of the mean energy and elastic collision rate follow this, as explained earlier. The main difference is in the ionization plots. Significantly larger numbers of ionizations are required for the discharge to be maintained in the case of oxygen due to the attachment. At the same time a higher field is required to compensate for the energy losses due to vibrational excitation. On the other hand, if we compare the plots for the far high pressure points in Figure 4, even on the first sight, they are quite different. While electrons in argon are concentrated equally at both halves of the gap at the same time and do not depart far from the center of the gap, in oxygen they are still almost reaching electrodes and form a continuous "zigzag" line. This is a consequence of a few times higher voltage required in the case of oxygen that leads to a much stronger force that pushes electrons. Also, small cut-offs in plots of the electron mean energy (and also to a lesser degree for elastic collisions) can be seen when the field changes its sign due to a more efficient energy relaxation in the molecular gas.

Finally, if we wish to isolate only the effect of attachment then we need to make simulation with oxygen with and without electron losses due to attachment. These results are shown in Figure 5. While differences are not as obvious as in the comparison between argon and oxygen it is clear that attachment narrows down the channel of electrons and of course the operating voltage needs to be higher. The electron losses remove electrons that are below the threshold of ionization. Electrons that are not accelerated by the field directly but go in the perpendicular or backward directions are more likely to be lost. One needs to bear in mind that all this occurs when electron energies are overlapping with ionization and thus only dissociative attachment with its high threshold is relevant and in competition with ionization.

3.3 Electron energy distribution functions

In Figure 6 electron energy distribution functions (EEDF) are presented for various initial conditions (p, V) along the breakdown-voltage curve for oxygen. Differently colored lines in the same figure (figures are marked with capital letters A–F) indicate different moments within one period of the RF field. Starting from A, there are obvious modulations of EEDFs at different phases of one period. As we move all the way to F, these modulations are still present, but less observable. A larger modulation from A to C can be explained by electron losses at electrodes, with varying times of arrival and numbers of electrons arriving at electrodes. The losses of electrons reaching the walls are for the highest energy electrons and, hence, a greater modulation of the EEDF develops.

For conditions related to the points D, E and F the swarm of electrons merely brushes the electrodes and only a small number of them is lost. At the same time their energies are low. Thus modulations of the EEDFs are less expressed (Fig. 6).

In Figure 6A at some instants of one time period the high energy tail of EEDFs reaches high energies. Due to a high applied voltage (Fig. 6A), there is a large energy transfer from the electric field to electrons. Also, as the pressure is low, electrons experience a small number of collisions in which they can lose energy. As a consequence, electrons gain a lot of energy very fast resulting in the long EEDF high-energy tail. Moving along the breakdown curve, the EEDF tails shrink from A to F. If we compare voltages at points A and F, they are not that much different. What really makes a difference is the pressure that is 4 times higher at the point F as compared to A. This leads to a higher number of collisions with oxygen molecules and more rapid energy relaxation.

Another valuable information that can be derived from the EEDF plots are the values of the electron mean energy and energy span. At point A the mean energy is around 10 eV and decreases as we move to F, where mean energy is close to 6 eV. These energies include the answer why the effect of the attachment is more obvious in the right-hand branch of the breakdown-voltage curve. As we know, the peak in the cross section for the two-body attachment process is around 6.6 eV. In the right-hand side of the breakdown-voltage curve, the peak of the cross section overlaps with the energies of the majority of electrons. In the left-hand side of the curve, due to a wider energy span, a significant number of electrons have energies above the peak of the cross sections for dissociative attachment and influence of that process is reduced. At the same time the effect of the three-body attachment, that peaks at low energies, is small for all conditions covered here [28].

One may conclude from Figure 6 that the crossover distributions indicated as C are more similar to those for the high pressure branch (D, E and F). Similar could be concluded for the spatial profiles shown in Figure 2 when it comes to the relative population of the electrons as they cross from one electrode to the other. Simply speaking growth as electrons cross the gap in 2c is small and more similar to the growth and radial extent in 2d–2f. On the other hand in 2c the overlap of the electron ensemble with electrodes is easily observed, it is sharp and similar to the lower pressure profiles 2a and 2b. Such overlap indicates a large number of electrons colliding with the surface and significant electron losses. As point 2c shows transition from one set of curves to the other in two major aspects it is a true transition point which leads to it being at the local minimum of the breakdown curves.

4 Conclusions

Since von Engel's theory of high-frequency breakdown, understanding of RF breakdown has not changed much. Von Engel explained the breakdown at low pressures when

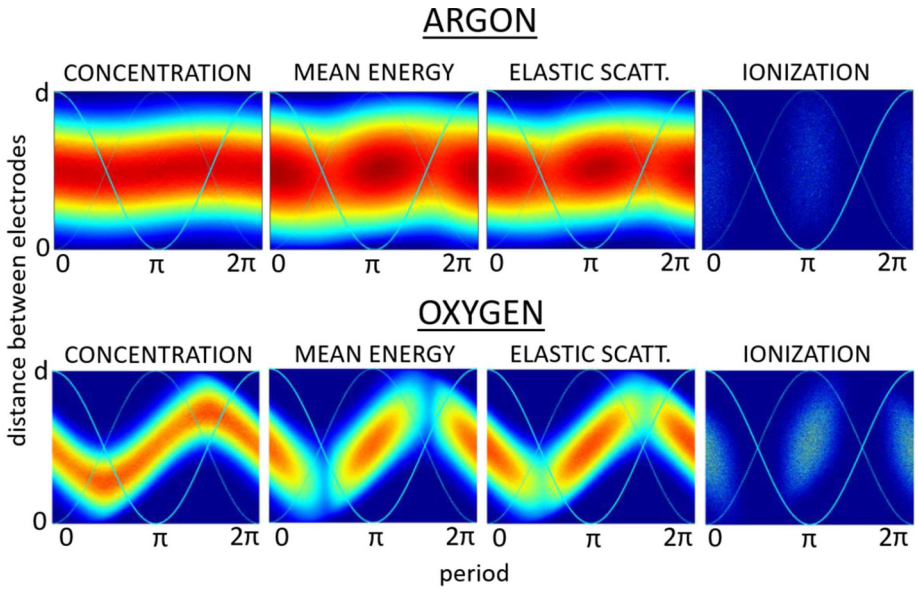

Fig. 4. Comparison of spatial profiles of electron concentration, mean energy and rates of elastic scattering and ionizations for two high pressure points presented in Figure 1. Argon: $V = 169\,\mathrm{V}$ and $p = 2.5\,\mathrm{Torr}$; oxygen: $V = 430\,\mathrm{V}$ and $p = 4.4\,\mathrm{Torr}$. X-axis of plots are periods of time from 0 to π, while y-axis are distances between electrodes from 0 to $d = 15\,\mathrm{mm}$. In both cases sampling time is the same, so that quantitative comparison can be made.

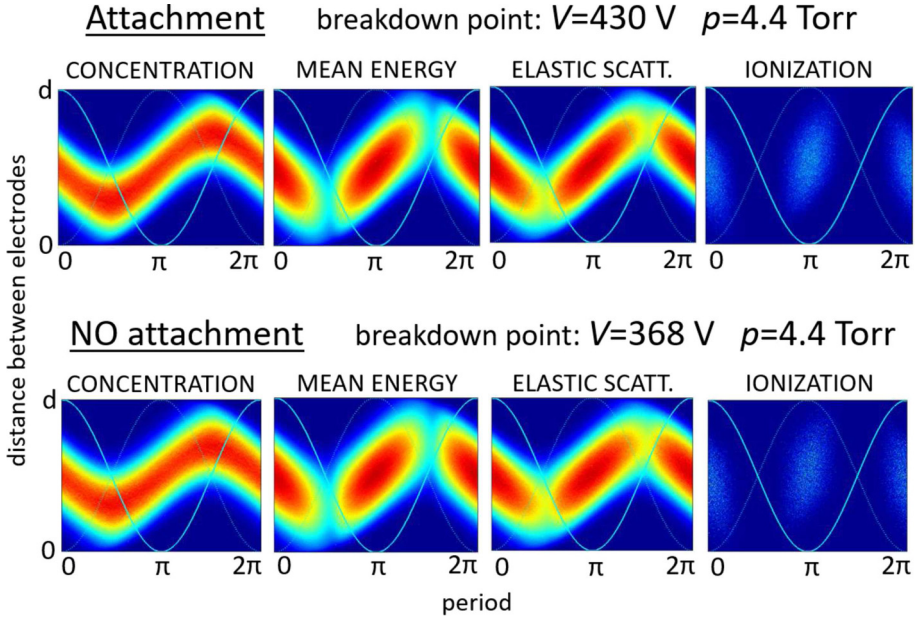

Fig. 5. Comparison of the attachment influence on the breakdown conditions observed in two cases: when attachment processes are included (breakdown conditions are $V = 430\,\mathrm{V}$ and $p = 4.4\,\mathrm{Torr}$) and when there are no attachments (breakdown conditions $V = 368\,\mathrm{V}$ and $p = 4.4\,\mathrm{Torr}$). Background gas is oxygen, frequency is 13.56 MHz and distance between electrodes is 15 mm.

electrons are reaching the electrodes, but at the same time he only superficially mentioned the influence of electrodes on the breakdown, with a conclusion that a more detailed swarm analysis is needed in the regions where electrons are not in contact with electrodes. We have tried to perform such an analysis in the case of argon in our previous papers [7,8]. We have done so by employing a Monte Carlo computational code and by using the fact that the beginning of the breakdown can be observed as a growth of an electron swarm in a time-varying electric field. RF breakdown in oxygen is an obvious step towards understanding the breakdown in electronegative gases. Comparison with argon pointed out differences between the two gases (one of which is electronegative). It was shown that vibrational energy losses change the operation of the RF breakdown considerably. To the left of the breakdown

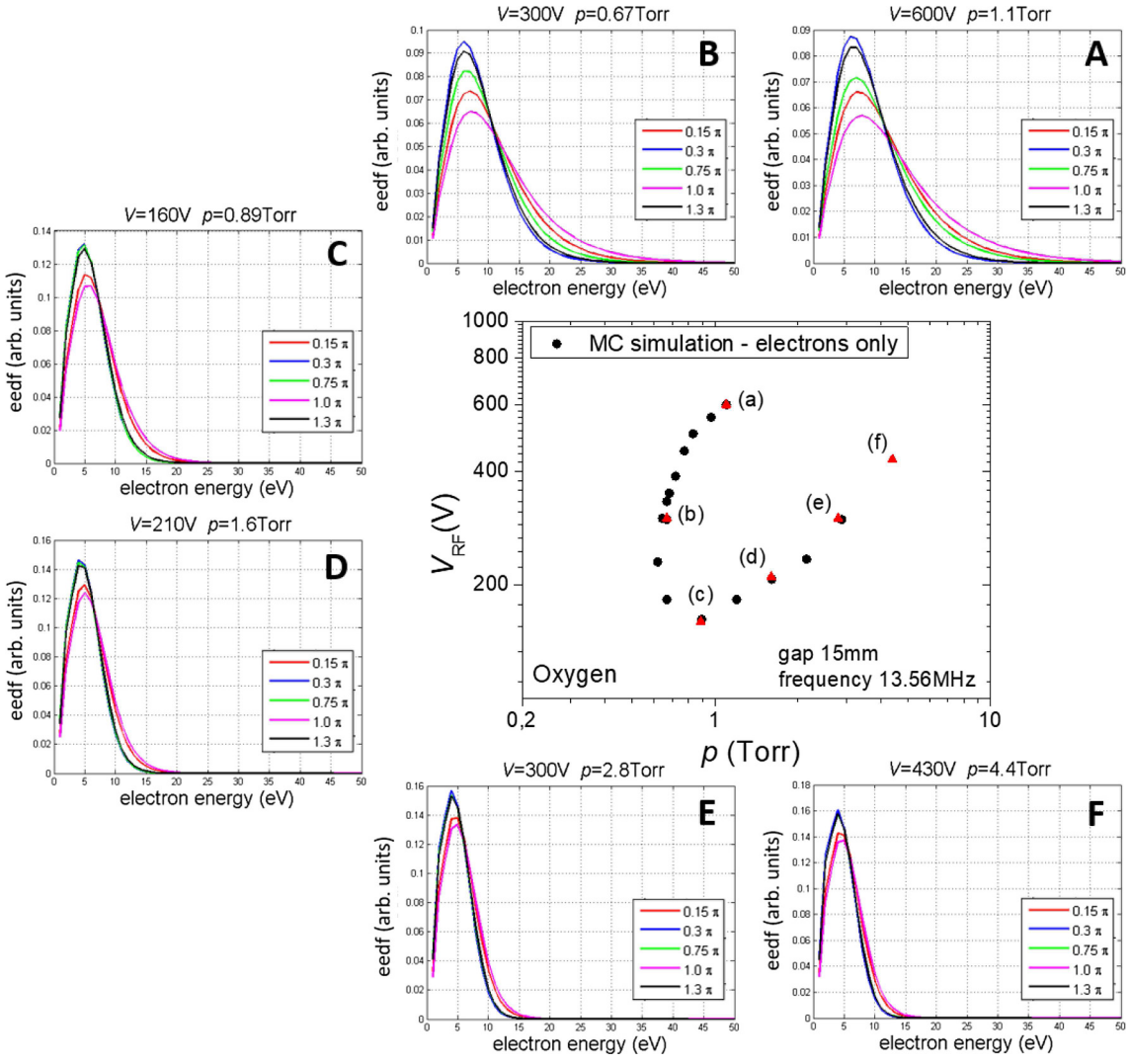

Fig. 6. EEDFs along breakdown-voltage curve for oxygen as background gas at frequency of 13.56 MHz and distance between electrodes of 15 mm. Different curves represent different phases of RF period and their variation indicates modulation in the distribution at different energies.

curve minimum one can observe similar behavior in two gases as most of the ionization occurs right in front of the electrodes and with significant losses to the electrodes. At pressures higher than those for the minimum a combination of vibrational energy losses and attachment drives breakdown to higher voltages and at the same time the required distance to achieve sufficient ionizations is longer and electrons approach closer to the electrodes while their radial width is smaller as the electrons going in perpendicular direction and backwards are more likely to be lost in attachment. Yet even under those conditions the number of electrons being lost at the electrodes is small. Finally, by observing EEDFs at different points on the breakdown curve and at different times over one period, processes of attachment have been indicated as responsible for a significant increase of the voltage in the right-hand side branch of the breakdown curve. At the same time the attachment has negligible influence on the left-hand side branch. Electron energies at high pressures overlap much more with cross sections for attachment, while at low pressures, the peak of EEDF exceeds energies where attachment has the greatest probability.

While the definition of the breakdown coincides with the conditions of the predominance of swarms, the study of the breakdown has a relevance for application of RF plasmas including pulsing [30,31] in processing and production of non-equilibrium (cold) plasmas at the atmospheric pressure [4,32] and [33]. In both examples, the presence of electronegative gases is unavoidable and conditions for the breakdown will significantly affect the required power supplies and operation of plasma devices. At the same time, the continued growth from the breakdown towards the formation of plasma may be followed by a more complex tools such as PIC [5,34] and [35]. By the same logic, the understanding of the afterglow has the same importance and requires a similar, albeit inverted, sequence of modeling.

The authors acknowledge support from the Serbian Ministry of Education, Science and Technological Development under project numbers OI 171037 and III 41011. ZLjP is grateful to Serbian Academy of Sciences and Arts and its project F155 for its partial support.

Author contribution statement

Marija Puač – put together the computational code and performed computational analysis, analysed the results and wrote the first draft of the manuscript. Antonije Đorđević – helped in planning, in the analysis of the results and worked on finalization of the manuscript. Zoran Lj Petrović – defined the plan of research, defined algorithms for the Monte Carlo code and worked on development of the RF breakdown model. He supervised the studies and analysis of the results, organization and finalization of the manuscript.

References

1. I. Adamovich, S.D. Baalrud, A. Bogaerts, P.J. Bruggeman, M. Cappelli, V. Colombo, U. Czarnetzki, U. Ebert, J.G. Eden, P. Favia, D.B. Graves, S. Hamaguchi, G. Hieftje, M. Hori, I.D. Kaganovich, U. Kortshagen, M.J. Kushner, N.J. Mason, S. Mazouffre, S. Mededovic Thagard, H.-R. Metelmann, A. Mizuno, E. Moreau, A.B. Murphy, B.A. Niemira, G.S. Oehrlein, Z.Lj. Petrović, L.C. Pitchford, Y.-K. Pu, S. Rauf, O. Sakai, S. Samukawa, S. Starikovskaia, J. Tennyson, K. Terashima, M.M. Turner, C.M.M. van de Sanden, A. Vardelle, J. Phys. D: Appl. Phys. **50**, 323001 (2017)
2. T. Makabe, Z.Lj. Petrović, in *Plasma Electronics: Applications in Microelectronic Device Fabrication*, 2nd edn. (CRC Taylor & Franics Group, Boca Raton, USA, 2015)
3. N. Puač, N. Škoro, K. Spasić, S. Živković, M. Milutinović, G. Malović, Z.Lj. Petrović, Plasma Process Polym. **15**, e1700082 (2017)
4. N. Puač, M. Gherardi, M. Shiratani, Plasma Process Polym. **15**, e1700174 (2018)
5. Z. Donko, Plasma Sourc. Sci. Tech. **20**, 024001 (2011)
6. M.J. Kushner, J. Phys. D: Appl. Phys. **42**, 194013 (2009)
7. M. Savić, M. Radmilovic-Radjenovic, M. Šuvakov, S. Marjanović, D. Marić, Z.Lj. Petrović, IEEE Trans. Plasma Sci. **39**, 2556 (2011)
8. M. Puač, D. Marić, M. Radmilović-Radjenović, M. Šuvakova, Z.Lj. Petrović, Plasma Sources Sci. Technol. **27**, 075013 (2018)
9. I. Korolov, A. Derzsi, Z. Donko, J. Phys. D: Appl. Phys. **47**, 475202 (2014)
10. I. Korolov, Z. Donko, Phys. Plasmas **22**, 093501 (2015)
11. T. Holstein, Phys. Rev. **70**, 367 (1946)
12. H. Margenau, Phys. Rev. **73**, 297 (1948)
13. H. Margenau, L.M. Hartman, Phys. Rev. **73**, 309 (1948)
14. H. Margenau, Phys. Rev. **73**, 326 (1948)
15. L.M. Hartman, Phys. Rev. **73**, 316 (1948)
16. E.W. Gill, A. von Engel, Proc. R. Soc. A **192**, 446 (1948)
17. E.W. Gill, A. von Engel, Proc. R. Soc. A **197**, 107 (1949)
18. V.A. Lisovskiy, V.D. Yegorenkov, J. Phys. D: Appl. Phys. **31**, 3349 (1998)
19. Z.Lj. Petrović, A. Đorđević, J. Petrović, J. Sivoš, M. Puać, G. Malović, D. Marić, in *82nd IUVSTA Workshop* (Okinawa, Japan, 2017), p. O2
20. J. Petrović, A. Đorđević, D. Marić, Z.Lj. Petrović, in *XXIV ESCAMPIG* (Glasgow, Scotland, 2018), p. 381
21. Y. Itikawa, J. Phys. Chem. Ref. Data **38**, 1 (2009)
22. Z. Ristivojevic, Z.Lj. Petrović, Plasma Sources Sci. Technol. **21**, 035001 (2012)
23. Z.Lj. Petrović, S. Bzenic, J. Jovanovic, S. Durovic, J. Phys. D: Appl. Phys. **28**, 2287 (1995)
24. A.V. Phelps, Z.Lj. Petrović, Plasma Sources Sci. Technol. **8**, R21 (1999)
25. PHELPS database, www.lxcat.net (Retrieved on May 29, 2015)
26. R.D. White, R.E. Robson, K.F. Ness, T. Makabe, J. Phys. D: Appl. Phys. **38**, 997 (2005)
27. S. Dujko, R.D. White, Z.Lj. Petrović, R.E. Robson, Plasma Sources Sci. Technol. **20**, 024013 (2011)
28. S. Dujko, U. Ebert, R.D. White, Z.Lj. Petrović, Jpn. J. Appl. Phys. **50**, 08JC01 (2011)
29. V. Lisovkiy, J.-P. Booth, K. Landry, D. Douai, J. Phys. D: Appl. Phys. **39**, 660 (2006)
30. K. Maeshige, G. Washio, T. Yagisawa, T. Makabe, J. Appl. Phys. **91**, 9494 (2002)
31. T. Ohmori, T.K. Goto, T. Makabe, Appl. Phys. Lett. **83**, 4637 (2003)
32. N. Škoro, N. Puač, S. Živković, D. Krstić-Milošević, U. Cvelbar, G. Malović, Z.Lj. Petrović, Eur. Phys. J. D **72**, 2 (2018)
33. E. Traldi, M. Boselli, E. Simoncelli, A. Stancampiano, M. Gherardi, V. Colombo, G.S. Settles, EPJ Tech. Instrum. **5**, 4 (2018)
34. M.M. Turner, A. Derzsi, Z. Donko, S.J. Kelly, T. Lafleur, T. Massenbrock, Phys. Plasmas **20**, 013507 (2013)
35. Z. Donko, Phys. Rev. E **57**, 7126 (1998)